

Correlations Between Quantumness and Learning Performance in Reservoir Computing with a Single Oscillator

Arsalan Motamedi,^{1,*} Hadi Zadeh-Haghighi,^{2,†} and Christoph Simon^{2,‡}

¹*Institute for Quantum Computing, Department of Physics & Astronomy University of Waterloo, Waterloo, ON, N2L 3G1, Canada*

²*Department of Physics and Astronomy, Institute for Quantum Science and Technology, Quantum Alberta, and Hotchkiss Brain Institute, University of Calgary, Calgary, AB T2N 1N4, Canada*

(Dated: April 10, 2023)

We explore the power of reservoir computing with a single oscillator in learning time series using quantum and classical models. We demonstrate that this scheme learns the Mackey-Glass (MG) chaotic time series, a solution to a delay differential equation. Our results suggest that the quantum nonlinear model is more effective in terms of learning performance compared to a classical nonlinear oscillator. We develop approaches for measuring the quantumness of the reservoir during the process. We prove that Lee-Jeong’s measure of macroscopicity is a non-classicality measure, and use it along with the Wigner negativity in our study of quantumness. We note that the evaluation of the Lee-Jeong measure is computationally more efficient than the Wigner negativity. Interestingly, we observe correlations between non-classicality and training accuracy in learning the MG series, suggesting that quantumness could be a valuable resource in reservoir computing. We, moreover, discriminate quantumness from complexity (dimensionality), and show that quantumness correlates more strongly with learning performance.

I. INTRODUCTION

The theory of quantum information processing has been thriving over the past few decades, offering various advantages, including efficient algorithms for breaking Rivest–Shamir–Adleman (RSA) encryption, exponential query complexity speed-ups, improvement of sensors and advances in metrology, and the introduction of secure communication protocols [1–8]. Nevertheless, the challenge of error correction and fault-tolerant quantum computing is still the biggest obstacle to the realization of a quantum computer. Despite threshold theorems giving the hope of fault-tolerant computation on quantum hardware [9–12], a successful realization of such methods is only recently accomplished on intermediate-size quantum computers [13], and the implementation of a large scale quantum computer is yet to be achieved. Moreover, today’s quantum hardware contain only a few tens of qubits. Hence we are in the noisy intermediate-scale quantum (NISQ) era, and it is of interest to know what tasks could be performed by such limited noisy devices that are hard to do with classical computers [14–17].

In the past few years, and on the classical computing side, neuromorphic (brain-inspired) computing has shown promising results [18–21], most notably the celebrated artificial neural networks used in machine learning. Neuromorphic computing uses a network of neurons to access a vast class of parametrized non-linear functions. Despite being very successful in accuracy, these

models are hard to train due to the need to optimize many parameters. Another obstacle in the training of such models is the vanishing gradient problem [22, 23].

A subfield of brain-inspired computing, derived from recurrent neural networks, is reservoir computing, where the learning is to be performed only at the readout. Notably, this simplification - optimizing over a smaller set of parameters - allows for circumventing the problem of barren plateaus encountered in the training of recurrent neural networks. Despite such simplifications, reservoir computing still shows remarkable performance [24–29]. Reservoir computing methods are often applied to temporal categorization, regression, and also time series prediction [30, 31]. Notably, there have been successful efforts on the physical implementation of (classical) reservoir computing [26, 29, 32].

More recently, the usefulness of quantum computing in the field of machine learning has been studied [33–35]. In addition to that, there are novel attempts to introduce an appropriate quantum counterpart for classical neuromorphic (in particular reservoir) computing. There have been different reservoir models considered, which could mostly be categorized as spin-based or oscillator-based [36–40] (corresponding to finite and infinite dimensional Hilbert spaces).

On the quantum reservoir computing front, there have been efforts such as [37], where one single Kerr oscillator is exploited for fundamental signal processing tasks. The approach used in [40] for quantum reservoir computing introduces non-linearity through the encoding of input signals in Gaussian states. Their approach has been proven to be universal, meaning that it can accurately approximate fading memory functions with arbitrary precision. [41] predicts time series using a spin-based model. [42] exploits a network of interacting quan-

* arsalan.motamedi@uwaterloo.ca

† hadi.zadehhaghighi@ucalgary.ca

‡ csimo@ucalgary.ca

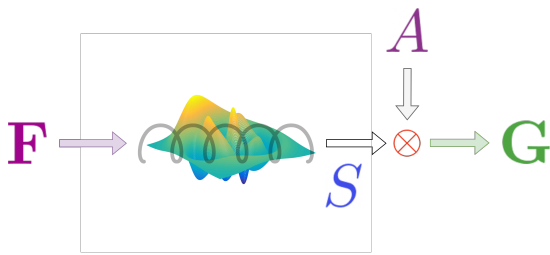


FIG. 1: A schematic representation of the computation model, either classical or quantum. In the learning process, we find the proper A that is to predict the sample set G , based on the outputs of the reservoir. The dynamics of the reservoir is controlled via sample set F .

tum reservoirs for tasks like quantum state preparation and tomography. [43] proposes heuristic approaches for optimized coupling of two quantum reservoirs. An analysis of the effect of quantumness is performed in [37], where the authors consider dimensionality as a quantum resource. The effects of quantumness have been studied more concretely in [44], where they consider an Ising model as their reservoir and show that the dimension of the phase space used in the computation is linked to the system's entanglement. Also, [41] demonstrates that quantum entanglement might enhance reservoir computing. Specifically, they show that a quantum model with a few strongly entangled qubits could perform as well as a classical reservoir with thousands of perceptions, and moreover, performance declines when the reservoir is decomposed into separable subsets of qubits.

In this work, we explore how well a single quantum non-linear oscillator performs time series predictions. In particular, we are focused on the prediction of the Mackey-Glass (MG) time series [45], which is often used as a benchmark task in reservoir computing. We then investigate the role of quantumness in the quantum learning model. We use two quantumness measures, the Wigner negativity and the Lee-Jeong measure. The latter was originally introduced as a measure for macroscopicity, but here we demonstrate that it is a non-classicality measure as well. Using our approaches, we observe that quantumness correlates with learning performance, and that it does so more strongly than dimensionality.

The paper is organized as follows. In Section II we introduce the reservoir computing method used in this work. Section III A shows the performance of the method. Section III B analyzes the effect of quantumness measures on performance. Finally, Section IV provides a discussion of the findings.

II. RESERVOIR COMPUTING

In this work, we use the approach introduced by Govia et al. [37] to feed the input signal to the reservoir by manipulating the Hamiltonian. We describe the state of our quantum and classical systems using $\hat{\rho}$ and a , respectively. Let us consider a time interval of length

Δt that has been discretized with N equidistant points $t_1 < \dots < t_N$. We can expand this set by considering M future values $t_{N+1} < \dots < t_{N+M}$, which are also equidistantly distributed. It is worth noting that the interval $t_N - t_1$ is equal to Δt . Our objective is to estimate a set of future values of the function f , which is denoted by $G = (f(t_i))_{i=N+1}^M$, given the recent observations $F = (f(t_i))_{i=1}^N$. To this end, we evolve our system so that $\hat{\rho}(t_j)$ (respectively, $a(t_j)$) depends on $f(t_1), \dots, f(t_j)$. We then obtain observations $s(t_i) = \langle \hat{O} \hat{\rho}(t_i) \rangle$ for an observable \hat{O} (respectively, $s(t_i) = (h \circ a)_i$ for a function h). Finally, we perform a linear regression on $(s(t_i))_{i=1}^N$ to predict G . In what follows we elaborate on the system's evolution in both classical and quantum cases.

For the classical reservoir, we consider the following evolution

$$\dot{a} = -iK(1 + 2|a|^2)a - \frac{\kappa}{2}a - i\alpha f(t) \quad (1)$$

with K , κ , and α being the reservoir's natural frequency, dissipation rate, and the amplifier of the input signal, respectively. We let $s(t) = \tanh(\text{Re}\{a(t)\})$. The quantum counterpart of the evolution described by Eq. (1) is the following Markovian dynamics [37, 46]

$$\begin{aligned} \frac{d}{dt}\hat{\rho}(t) &= -i[\hat{H}(t), \hat{\rho}(t)] + \kappa \mathcal{D}_a(\hat{\rho}) \\ \text{where } \hat{H}(t) &= K \hat{N}^2 + \alpha f(t) \hat{X}, \\ \text{and } \mathcal{D}_a(\hat{\rho}) &= \hat{a}\hat{\rho}\hat{a}^\dagger - \{\hat{N}, \hat{\rho}\}/2. \end{aligned} \quad (2)$$

Note that we use the properly scaled parameters, such that the uncertainty principle becomes $\Delta x \Delta p \geq 1/2$. The parameters (α, κ, K) are the same as above (in (1)). The operators \hat{X} , \hat{a} , and \hat{N} represent the position, annihilation, and the number operator respectively. We let $s(t) = \text{tr}(\hat{\rho}(t) \tanh \hat{X})$. Utilizing the non-linear quantum evolution (2) as our quantum reservoir, we perform the learning of the MG time series.

Let us now provide details on the process of linear regression. Our objective is to find the predictor A that satisfies the relationship $G \approx As$ (note that we think of G and s as column vectors). To this end, we conduct the experiment T times and collect the resulting column vectors as $\vec{s}_1, \vec{s}_2, \dots, \vec{s}_T$. We then define a matrix \mathbf{S} as the concatenation of these column vectors

$$\mathbf{S} := (s_1 | s_2 | \dots | s_T) \quad (3)$$

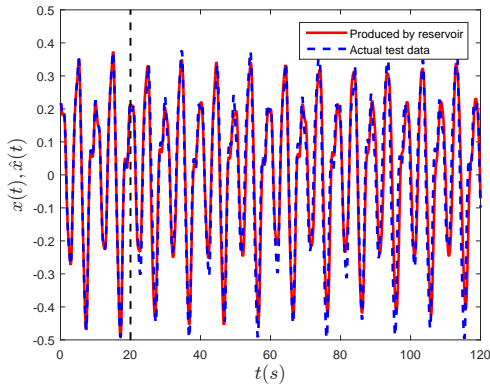
Similarly, we define the matrix \mathbf{G} as

$$\mathbf{G} := (G_1 | G_2 | \dots | G_T). \quad (4)$$

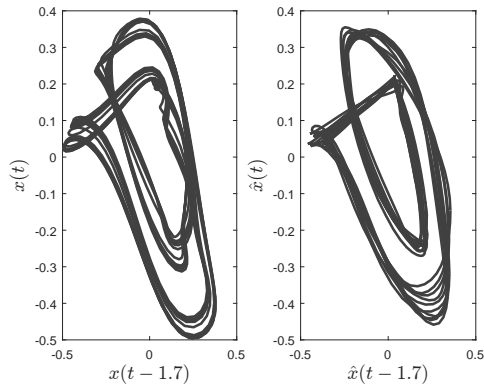
Finally, we choose A by applying Tikhonov regularization [47], which results in the following choice of A

$$A = \mathbf{G}\mathbf{S}^T(\mathbf{S}\mathbf{S}^T + \gamma\mathbb{I})^{-1} \quad (5)$$

with γ and \mathbb{I} being a regularization parameter, and the identity matrix, respectively. One should note that \mathbf{G} ,



(a) The oscillator is trained to reproduce the Mackey-Glass time series, and then predict, given initial values, which are the data points before the dashed line. The parameters in (2) are chosen as $(\alpha, \kappa, K) = (1.2, 0.1, 0.05)$.



(b) Comparing the delayed embedding of the actual Mackey-Glass series (left) with that of the reservoir's output (right). See Section III A for definitions.

FIG. 2: Performance of the trained quantum model.

and \mathbf{S} written in (5) correspond to T training samples that we take. The matrix A evaluated above is then used for the prediction of the test data. Fig. 1 provides a schematic representation of the reservoir training.

Overall, to predict time series, the reservoir is initially trained to determine A by using equation (5). After training, a set of initial values outside of the training data is inputted into the oscillator. The oscillator uses A to predict future values, which are then used as initial values for further predictions.

III. RESULTS

This section investigates the performance of a single Kerr non-linear oscillator trained on the MG chaotic time series, as well as the effect of different quantumness measures on the performance of the reservoir. Specifically, in Section III A, we discuss how well the non-linear oscillator could learn when trained on chaotic time series, while in Section III B, we examine the impact of various quantumness measures. Lastly, we outline further investigations, including the effects of noise.

To simulate quantum dynamics in the Fock space, we truncate every operator in the number basis, making them d_t -dimensional. Notably, the simulation results in this work use a dimension $d_t \geq 20$, which is sufficiently large as most of the states considered have a significant overlap with the subspace spanned by the number states $|n\rangle$ for $n \leq 10$ (For instance, we use the coherent state $|\alpha\rangle$ with $\alpha = 1 + i$, the overlap of which with the first 20 Fock states is larger than $1 - 6.5 \times 10^{-15}$).

A. Learning Time Series

In what follows we report the results obtained by training our single non-linear oscillator. Here, we consider the prediction the chaotic MG series. MG is formally defined as the solution to the following delay differential equation

$$\dot{x}(t) = \beta \frac{x(t - \tau)}{1 + x(t - \tau)^n} - \gamma x(t). \quad (6)$$

We use the parameters $\beta = 0.2$, $\gamma = 0.1$, $n = 10$, and $\tau = 17$ throughout this work. The performance of the trained reservoir on the test data is presented in Fig. 2a. Fig. 2b shows the delayed embedding of the predicted MG, which is compared to the actual diagram. One can readily observe that this model is successful in learning MG.

B. Quantumness

In this section, we introduce our quantumness measure and study the effect of quantumness on that basis on the accuracy of the learning model.

1. Quantumness Measures

Our main goal here is to determine if there is a correlation between the quantumness of the system and the accuracy of the learning process. An affirmative answer would be a quantum advantage for this computational model. To this end, we need to quantify the quantumness of a state in Fock space. We point out that there has been extensive research done on the quantification of quantumness [48–50]. Furthermore, there has been a line of research in the study of the macroscopicity of quantum

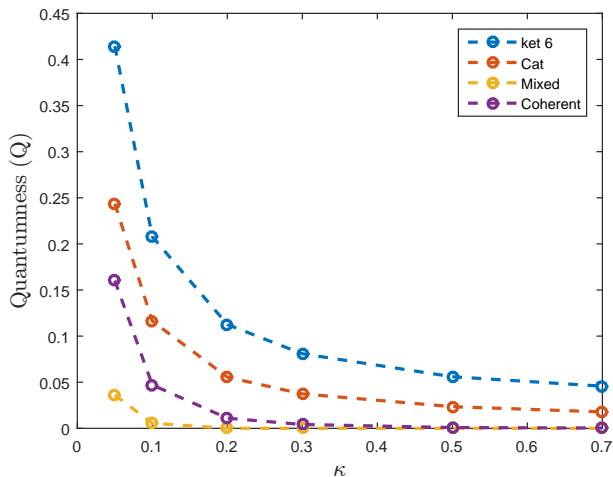


FIG. 3: Average quantumness (Q) during the evolution is shown to be decreasing as κ (the photon loss rate) increases. The states used as initial states are the mixed state (labeled as ‘mix’) being proportional to $|\alpha\rangle\langle\alpha| + |-\alpha\rangle\langle-\alpha|$, the corresponding ‘cat’ state being proportional to $|\alpha\rangle + |-\alpha\rangle$, and the $|6\rangle$ (‘ket 6’). The parameters are $(\alpha, \lambda, K) = (1.2, 0.1, 0.05)$, where λ is the pumping parameters, used to keep all the quantumness values in a similar range.

states and their effective size [51–54]. One such measure in the Fock space is defined by Lee and Jeong [55] as follows:

$$I(\hat{\rho}) := \pi \left(\int_{x,p} (\partial_x W(x,p))^2 + (\partial_p W(x,p))^2 - 2W(x,p)^2 \right) \quad (7)$$

where x, p are dimensionless space and momentum components (in such scale, the uncertainty principle becomes $\Delta x \Delta p \geq 1/2$). This formulation can also be found in [56]. The following identities are pointed out in [55]:

- $I(|\alpha\rangle\langle\alpha|) = 0$, for any coherent state $|\alpha\rangle$.
- $\forall n \in \mathbb{N} : I(\sum_{i=0}^{n-1} \frac{1}{n} |i\rangle\langle i|) = 0$, where $|i\rangle$ are the Fock states (i.e., the eigen-vectors of the number operator).

It is worth mentioning that this measure can obtain negative values [56]. Intuitively, one could think of $I(\hat{\rho})$ as the fineness of the Wigner function associated with $\hat{\rho}$. The aforementioned results may suggest that the positiveness of I indicates non-classicality, as the coherent state and a diagonal density matrix in the Fock basis are considered as classical states. In the following theorem, we prove that if $I(\hat{\rho}) > 0$, then ρ cannot be written as a mixture of coherent states, hence being non-classical.

Theorem 1. *If $\hat{\rho}$ is a mixture of coherent states, then $I(\hat{\rho}) \leq 0$.*

The proof is provided in Appendix C. One should also note that I is computable in a much shorter time as it

reformulated as ([55])

$$I(\hat{\rho}) = \text{tr}(\hat{\rho} \mathcal{D}_a(\hat{\rho})). \quad (8)$$

On the other hand, the computation of Wigner negativity with the current algorithms is costly, as it requires the computation of the entire Wigner function. We hence use the following quantumness measure Q

$$Q(\hat{\rho}) = \begin{cases} I(\hat{\rho}) & \text{if } I(\hat{\rho}) > 0, \\ 0 & \text{o.w.} \end{cases} \quad (9)$$

We make this choice as we do not want our quantumness measure to obtain negative values. We observe that this measure is consistent with some intuitions regarding the quantumness of reservoir computing, which have been previously used in [37]. In particular, the intuition that by increasing κ we should reach a classical limit, which is illustrated in Fig. 3. Finally, we point out the fact that the quantumness of the state changes during evolution. This is indeed observed in Fig. 4.

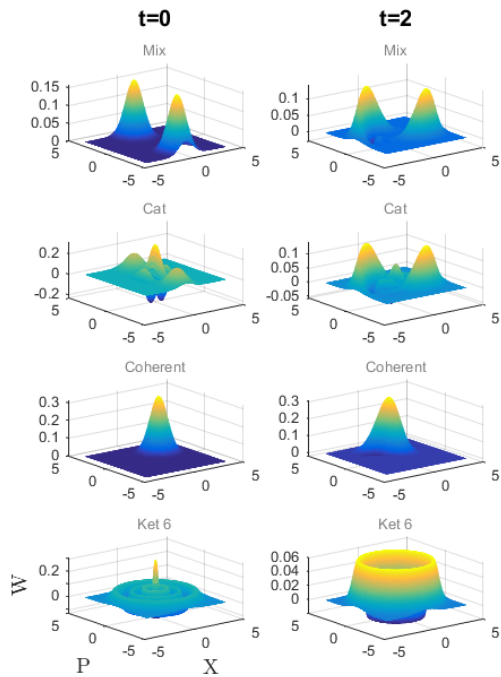
2. Example States

To study the quantumness effect, here, we used different initial states. For instance, we considered training the reservoir initialized at different states including the cat state (i.e., normalized $|\alpha\rangle + |-\alpha\rangle$), the corresponding mixed state (i.e., normalized $|\alpha\rangle\langle\alpha| + |-\alpha\rangle\langle-\alpha|$), the coherent state $|\alpha\rangle$, and the number state $|n\rangle$. We further added the data obtained from the training of a classical model. We changed the training data sizes to better compare different states and models. The result is presented in Fig. 5. Despite not showing a significant advantage for states with high quantumness, this diagram reveals that the quantum model for the reservoir outperforms the classical model in the task of MG prediction.

3. Random States

Since the distinction between our examples in Fig. 5 does not demonstrate a clear correlation between the quantumness and the performance, we pick random states and scrutinize the correlations between the training accuracy and quantumness measures. Interestingly, Fig. 6b shows a clear correspondence between the quantumness and the performance; providing us with a piece of evidence that the quantumness does indeed help achieve more precise predictions. For the initial random states, we fix a dimension d , then pick a state according to the Haar random measure on $\mathcal{H}(\mathbb{C}^d)$ [57]. To this end, we use [58, Proposition 7.17]. In particular, we consider the set of $2d$ independent and identically distributed (i.i.d.) standard Gaussian random variables $X_1, Y_1, \dots, X_d, Y_d$ to construct the state

$$|\psi\rangle = \frac{(X_1 + \iota Y_1, \dots, X_d + \iota Y_d)}{\sqrt{\sum_i X_i^2 + Y_i^2}} \quad (10)$$



(a) Two snapshots of Wigner functions of the reservoir's state, starting from different states. The plots correspond to the initial state being the mixed state (top), cat state (middle), and the number state $|6\rangle$ (bottom).

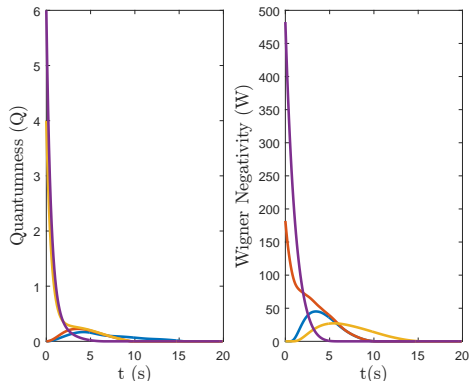


FIG. 5: Training curves for both classical and quantum models. Different initial states for the quantum model have been considered. Those are the mixed state (labeled as 'mix') being proportional to $|\alpha\rangle\langle\alpha| + |-\alpha\rangle\langle-\alpha|$, the corresponding 'cat' state being proportional to $|\alpha\rangle + |-\alpha\rangle$, the coherent state $|\alpha\rangle$, and the number state $|6\rangle$ ('ket 6'). The oscillator parameters are $(K, \kappa, \alpha) = (1.2, 0.1, 0.05)$.

(b) Quantumness (Q) during the evolution. The label 'mix' corresponds to the case where the initial state is $|\alpha\rangle\langle\alpha| + |-\alpha\rangle\langle-\alpha|$, the label 'cat' corresponds to $|\alpha\rangle + |-\alpha\rangle$, and the label 'ket6' corresponds to $|6\rangle$ (Note that the correspondences are up to a normalization factor). The values are normalized by the absolute maximum in each diagram.

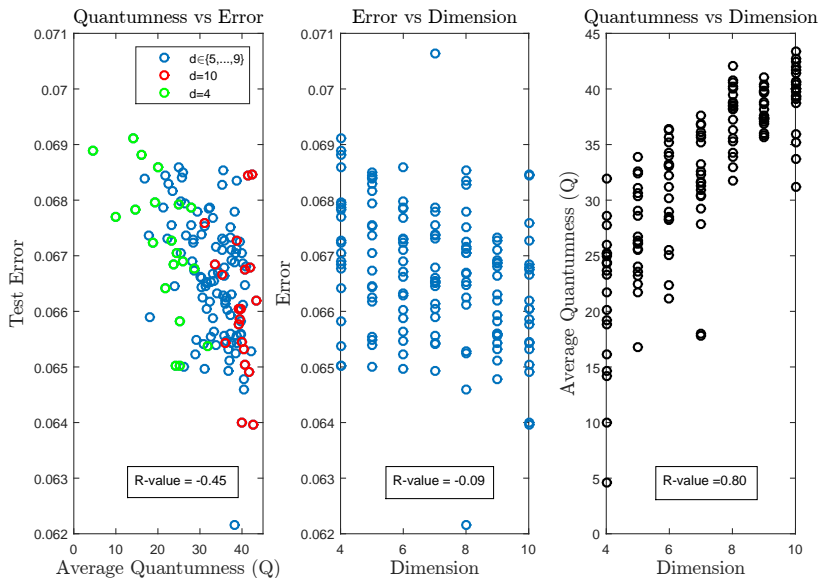
FIG. 4: Quantumness and Wigner plots of the reservoir's state evolution. The oscillator parameters are $(\alpha, \kappa, K) = (1.2, 0.1, 0.05)$.

which is a Haar random state in $\mathcal{H}(\mathbb{C}^d)$. To more elaborate, according to [58, Proposition 7.17], the distribution of the states generated by (10), are invariant under the action of the unitaries acting on $\mathcal{H}(\mathbb{C}^d)$. We repeated this random state generation for $d = 4$ to $d = 10$, collecting 20 samples for each dimension, and truncated the Fock space by considering the subspace spanned by the first 25 number states (i.e., $d_t = 25$) to obtain the results pre-

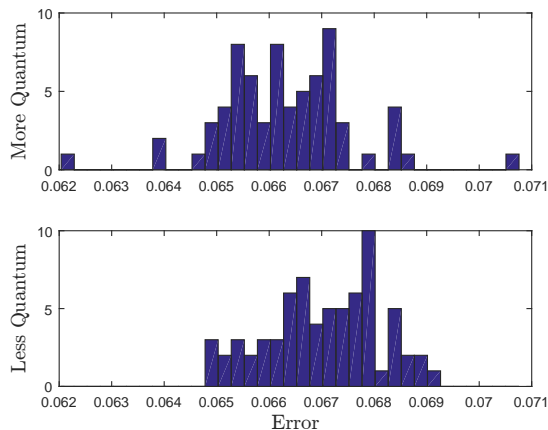
sented in Fig. 6a. We emphasize that the same training protocol is applied to all such states in every dimension.

The correlation coefficients of the data show a relationship between the quantumness and the training accuracy. We further investigated the effects of quantumness using the t-tests. Our hypothesis test (Fig. 6b) resulted in a p -value of 2.1×10^{-4} . As a reminder, the p -value in our case of study is an estimation of a lower bound on the probability of observing the obtained results under the hypothesis that the quantumness has no positive effect on the training accuracy. Thus, such a small p -value confirms the efficacy of quantumness on the training outcome. We further investigate the relation of dimensionality with the error. We note that increasing the dimension used for the oscillator could be understood as increasing the complexity and the power of the model. From Fig. 6a we observe that although dimensionality correlates well with quantumness, it does not correlate much with accuracy. This suggests that quantumness is a more effective factor than complexity.

A similar analysis is presented in Appendix A, where we consider the Wigner negativity as our quantumness measure. Other than that, we also investigate the robustness of the model by introducing a variety of noises to the evolution. Our results, presented in Appendix B, suggest that the model can tolerate a considerable amount of noise.



(a) **Correlation between test error, quantumness and dimensionality of the reservoir.** We observe a strong correlation between quantumness and performance accuracy (left). We see no strong correlation between dimensionality and the training error (middle). We observe a strong correlation between quantumness and dimensionality (right).



(b) Hypothesis test. We divide the data in half, based on the median. The ‘more quantum’ state corresponds to $Q > Q_{\text{median}}$, and the ‘less quantum’ corresponds to $Q < Q_{\text{median}}$. The p-value of this test is less than 2.1×10^{-4} , rejecting the null hypothesis. Meaning that the two data sets have different means.

FIG. 6: Training accuracy for the task of Mackey-Glass prediction, using 140 random states (20 datapoints for each $d = 4, \dots, 10$). We elaborate on the random selection process at the end of section III B.

IV. DISCUSSION

In this study, we focused on evaluating the effectiveness of a quantum non-linear oscillator in making time-series predictions and examining how quantumness impacts the quantum learning model. We utilize two quantumness metrics, namely the Wigner negativity and the Lee-Jeong measure [55]. The former is a widely accepted measure, while the latter was initially introduced to measure macroscopicity and in this work is shown to be a quantumness measure as well. Through our method-

ologies, we discovered that quantumness has a stronger correlation with performance than the dimensionality of the reservoir’s state. Overall, our findings contribute to a deeper understanding of the role of quantumness in continuous-variable reservoir computing and highlight its potential for enhancing the performance of this computational model.

Our work raises a number of important questions. Firstly, we aim to determine what specific structures within a reservoir computing model will lead to quantum speed-ups. Additionally, one can investigate the im-

pect of quantumness on a network of oscillators in future research. Notably, when dealing with a network of continuous variable oscillators, entanglement as a measure of quantumness could also be examined. It is worth mentioning that our method has potential for implementation on actual quantum hardware, and may even be feasible with current limited devices due to the strong Kerr non-linearity present in models for a transmon superconducting qubit [59].

V. CODE AVAILABILITY

The codes used for the generation of the plots of this manuscript are publicly available at <https://github.com/arsalan-motamedi/QRC>.

VI. ACKNOWLEDGEMENT

We acknowledge Wilten Nicola for fruitful discussions and for reading and commenting on an earlier version

of the manuscript. The authors acknowledge an NSERC Discovery Grant, the Alberta Major Innovation Fund, Alberta Innovates, Quantum City, and NRC CSTIP grant AQC 007.

VII. CONTRIBUTIONS

All authors contributed extensively to the presented work. H.Z-H. and C.S. conceived the original ideas and supervised the project. A.M. performed analytical studies and numerical simulations and generated different versions of the manuscript. H.Z-H. and C.S. verified the calculations, provided detailed feedback on the manuscript, and applied many insightful updates.

-
- [1] P. W. Shor, Polynomial-time algorithms for prime factorization and discrete logarithms on a quantum computer, *SIAM review* **41**, 303 (1999).
- [2] E. R. MacQuarrie, C. Simon, S. Simmons, and E. Maine, The emerging commercial landscape of quantum computing, *Nature Reviews Physics* **2**, 596 (2020).
- [3] A. W. Harrow, A. Hassidim, and S. Lloyd, Quantum algorithm for linear systems of equations, *Physical Review Letters* **103**, 10.1103/physrevlett.103.150502 (2009).
- [4] M. A. Nielsen and I. Chuang, *Quantum computation and quantum information* (2002).
- [5] C. H. Bennett and G. Brassard, Quantum cryptography: Public key distribution and coin tossing, arXiv preprint arXiv:2003.06557 (2020).
- [6] C. L. Degen, F. Reinhard, and P. Cappellaro, Quantum sensing, *Reviews of modern physics* **89**, 035002 (2017).
- [7] C. Simon, Towards a global quantum network, *Nature Photonics* **11**, 678 (2017).
- [8] R. L. Rivest, A. Shamir, and L. M. Adleman, Cryptographic communications system and method (1983), uS Patent 4,405,829.
- [9] D. Aharonov and M. Ben-Or, Fault-tolerant quantum computation with constant error, in *Proceedings of the twenty-ninth annual ACM symposium on Theory of computing* (1997) pp. 176–188.
- [10] E. Knill, R. Laflamme, and W. H. Zurek, Resilient quantum computation, *Science* **279**, 342 (1998).
- [11] A. Y. Kitaev, Fault-tolerant quantum computation by anyons, *Annals of Physics* **303**, 2 (2003).
- [12] P. W. Shor, Fault-tolerant quantum computation, in *Proceedings of 37th conference on foundations of computer science* (IEEE, 1996) pp. 56–65.
- [13] R. Acharya, I. Aleiner, R. Allen, T. I. Andersen, M. Ansmann, F. Arute, K. Arya, A. Asfaw, J. Atalaya, R. Babush, *et al.*, Suppressing quantum errors by scaling a surface code logical qubit, arXiv preprint arXiv:2207.06431 (2022).
- [14] K. Temme, S. Bravyi, and J. M. Gambetta, Error mitigation for short-depth quantum circuits, *Physical review letters* **119**, 180509 (2017).
- [15] K. Bharti, A. Cervera-Lierta, T. H. Kyaw, T. Haug, S. Alperin-Lea, A. Anand, M. Degroote, H. Heimonen, J. S. Kottmann, T. Menke, *et al.*, Noisy intermediate-scale quantum algorithms, *Reviews of Modern Physics* **94**, 015004 (2022).
- [16] A. Kandala, K. Temme, A. D. Córcoles, A. Mezzacapo, J. M. Chow, and J. M. Gambetta, Error mitigation extends the computational reach of a noisy quantum processor, *Nature* **567**, 491 (2019).
- [17] J. Preskill, Quantum computing in the nisq era and beyond, *Quantum* **2**, 79 (2018).
- [18] E. Farquhar, C. Gordon, and P. Hasler, A field programmable neural array, in *2006 IEEE international symposium on circuits and systems* (IEEE, 2006) pp. 4–pp.
- [19] J. J. Hopfield, Neural networks and physical systems with emergent collective computational abilities., *Proceedings of the national academy of sciences* **79**, 2554 (1982).
- [20] J. Schmidhuber, Deep learning in neural networks: An overview, *Neural networks* **61**, 85 (2015).
- [21] I. Goodfellow, J. Pouget-Abadie, M. Mirza, B. Xu, D. Warde-Farley, S. Ozair, A. Courville, and Y. Bengio, Generative adversarial networks, *Communications of the ACM* **63**, 139 (2020).
- [22] R. Pascanu, T. Mikolov, and Y. Bengio, On the difficulty of training recurrent neural networks, in *International conference on machine learning* (PMLR, 2013) pp. 1310–1318.
- [23] S. Basodi, C. Ji, H. Zhang, and Y. Pan, Gradient amplification: An efficient way to train deep neural networks,

- Big Data Mining and Analytics **3**, 196 (2020).
- [24] W. Maass, T. Natschläger, and H. Markram, Real-time computing without stable states: A new framework for neural computation based on perturbations, *Neural computation* **14**, 2531 (2002).
- [25] H. Jaeger and H. Haas, Harnessing nonlinearity: Predicting chaotic systems and saving energy in wireless communication, *science* **304**, 78 (2004).
- [26] G. Tanaka, T. Yamane, J. B. Héroux, R. Nakane, N. Kanazawa, S. Takeda, H. Numata, D. Nakano, and A. Hirose, Recent advances in physical reservoir computing: A review, *Neural Networks* **115**, 100 (2019).
- [27] A. Röhm and K. Lüdge, Multiplexed networks: reservoir computing with virtual and real nodes, *Journal of Physics Communications* **2**, 085007 (2018).
- [28] W. Nicola and C. Clopath, Supervised learning in spiking neural networks with force training, *Nat Commun* **8**, [10.1038/s41467-017-01827-3](https://doi.org/10.1038/s41467-017-01827-3) (2017).
- [29] K. Nakajima, Reservoir computing: Theory, physical implementations, and applications, IEICE Technical Report; IEICE Tech. Rep. **118**, 149 (2018).
- [30] B. Schrauwen, D. Verstraeten, and J. Van Campenhout, An overview of reservoir computing: theory, applications and implementations, in *Proceedings of the 15th european symposium on artificial neural networks. p. 471-482 2007* (2007) pp. 471–482.
- [31] Y. D. Mammedov, E. U. Olugu, and G. A. Farah, Weather forecasting based on data-driven and physics-informed reservoir computing models, *Environmental Science and Pollution Research* **29**, 24131 (2022).
- [32] S. Kan, K. Nakajima, T. Asai, and M. Akai-Kasaya, Physical implementation of reservoir computing through electrochemical reaction, *Advanced Science* **9**, 2104076 (2022).
- [33] J. Biamonte, P. Wittek, N. Pancotti, P. Rebentrost, N. Wiebe, and S. Lloyd, Quantum machine learning, *Nature* **549**, 195 (2017).
- [34] F. P. Maria Schuld, Ilya Sinayskiy, An introduction to quantum machine learning, *Contemporary Physics* [10.1080/00107514.2014.964942](https://doi.org/10.1080/00107514.2014.964942).
- [35] M. Schuld, I. Sinayskiy, and F. Petruccione, An introduction to quantum machine learning, *Contemporary Physics* **56**, 172 (2015).
- [36] K. Fujii and K. Nakajima, Quantum reservoir computing: a reservoir approach toward quantum machine learning on near-term quantum devices, in *Reservoir computing* (Springer, 2021) pp. 423–450.
- [37] L. C. G. Góvia, G. J. Ribeill, G. E. Rowlands, H. K. Krovi, and T. A. Ohki, Quantum reservoir computing with a single nonlinear oscillator, *Phys. Rev. Research* **3**, [013077](https://doi.org/10.1103/PhysRevResearch.3.013077) (2021).
- [38] I. Luchnikov, S. Vintskevich, H. Ouerdane, and S. Filipov, Simulation complexity of open quantum dynamics: Connection with tensor networks, *Physical review letters* **122**, 160401 (2019).
- [39] R. Martínez-Peña, J. Nokkala, G. L. Giorgi, R. Zambrini, and M. C. Soriano, Information processing capacity of spin-based quantum reservoir computing systems, *Cognitive Computation* , 1 (2020).
- [40] J. Nokkala, R. Martínez-Peña, G. L. Giorgi, V. Parigi, M. C. Soriano, and R. Zambrini, Gaussian states of continuous-variable quantum systems provide universal and versatile reservoir computing, *Communications Physics* **4**, 53 (2021).
- [41] P. Pfeffer, F. Heyder, and J. Schumacher, Quantum reservoir computing of thermal convection flow, arXiv preprint arXiv:2204.13951 (2022).
- [42] S. Ghosh, K. Nakajima, T. Krisnanda, K. Fujii, and T. C. Liew, Quantum neuromorphic computing with reservoir computing networks, *Advanced Quantum Technologies* **4**, 2100053 (2021).
- [43] S. Vintskevich and D. Grigoriev, Computing with two quantum reservoirs connected via optimized two-qubit nonselective measurements, arXiv preprint arXiv:2201.07969 (2022).
- [44] N. Götting, F. Lohof, and C. Gies, Exploring quantum mechanical advantage for reservoir computing, arXiv preprint arXiv:2302.03595 (2023).
- [45] M. C. Mackey and L. Glass, Oscillation and chaos in physiological control systems, *Science* **197**, 287 (1977).
- [46] C. Gardiner, P. Zoller, and P. Zoller, *Quantum noise: a handbook of Markovian and non-Markovian quantum stochastic methods with applications to quantum optics* (Springer Science & Business Media, 2004).
- [47] S. Shalev-Shwartz and S. Ben-David, *Understanding machine learning: From theory to algorithms* (Cambridge university press, 2014).
- [48] B. Groisman, D. Kenigsberg, and T. Mor, "quantumness" versus "classicality" of quantum states, arXiv preprint quant-ph/0703103 (2007).
- [49] H. Ollivier and W. H. Zurek, Quantum discord: a measure of the quantumness of correlations, *Physical review letters* **88**, 017901 (2001).
- [50] K. Takahashi, Wigner and husimi functions in quantum mechanics, *Journal of the Physical Society of Japan* **55**, 762 (1986).
- [51] F. Fröwis, P. Sekatski, W. Dür, N. Gisin, and N. Sangouard, Macroscopic quantum states: Measures, fragility, and implementations, *Reviews of Modern Physics* **90**, 025004 (2018).
- [52] S. Nimmrichter and K. Hornberger, Macroscopicity of mechanical quantum superposition states, *Physical review letters* **110**, 160403 (2013).
- [53] A. J. Leggett and A. Garg, Quantum mechanics versus macroscopic realism: Is the flux there when nobody looks?, *Physical Review Letters* **54**, 857 (1985).
- [54] A. J. Leggett, Note on the "size" of schroedinger cats, arXiv preprint arXiv:1603.03992 (2016).
- [55] C.-W. Lee and H. Jeong, Quantification of macroscopic quantum superpositions within phase space, *Physical review letters* **106**, 220401 (2011).
- [56] J. Gong, [Comment on "quantification of macroscopic quantum superpositions within phase space"](https://arxiv.org/abs/1105.1322) (2011).
- [57] A. Haar, Der massbegriff in der theorie der kontinuierlichen gruppen, *Annals of mathematics* , 147 (1933).
- [58] J. Watrous, *The theory of quantum information* (Cambridge university press, 2018).
- [59] P. Bertet, F. Ong, M. Boissonneault, A. Bolduc, F. Mallet, A. Doherty, A. Blais, D. Vion, and D. Esteve, *Circuit quantum electrodynamics with a nonlinear resonator* (Oxford University Press, 2012).
- [60] R. L. Hudson, When is the wigner quasi-probability density non-negative?, *Reports on Mathematical Physics* **6**, 249 (1974).
- [61] A. Kenfack and K. Życzkowski, Negativity of the wigner function as an indicator of non-classicality, *Journal of Optics B: Quantum and Semiclassical Optics* **6**, 396

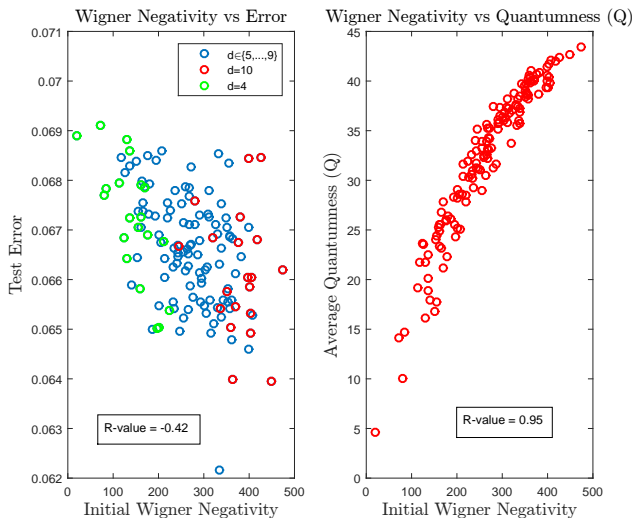


FIG. 7: The effects of Wigner negativity on the training performance. As observed, we get a correlation between Wigner negativity and test error, which again highlights the effect of quantumness. Moreover, we observe that there is a strong correlation between the quantumness measures considered in this work.

(2004).

- [62] T. Kubota, Y. Suzuki, S. Kobayashi, Q. H. Tran, N. Yamamoto, and K. Nakajima, [Quantum noise-induced reservoir computing](#) (2022).
- [63] D. Fry, A. Deshmukh, S. Y.-C. Chen, V. Rastunkov, and V. Markov, Optimizing quantum noise-induced reservoir computing for nonlinear and chaotic time series prediction, arXiv preprint arXiv:2303.05488 (2023).
- [64] O. E. Rössler, An equation for continuous chaos, *Physics Letters A* **57**, 397 (1976).
- [65] O. Rossler, An equation for hyperchaos, *Physics Letters A* **71**, 155 (1979)

Appendices

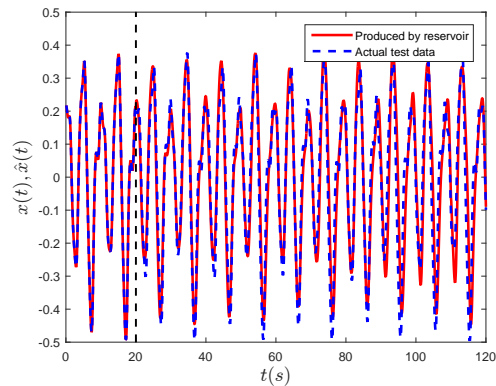
A. COMPARISONS WITH WIGNER NEGATIVITY

In this appendix, we examine the quantumness of the system by Wigner negativity. We recall that the Wigner negativity is the volume under the $W = 0$ plane for a Wigner function, and is often considered as a quantumness measure in the literature [60, 61]. The computation of Wigner negativity is more costly than the Lee-Jeong measure introduced in Section III B 1. Hence, we only compute it for the initial state. The result of this study is presented in Fig. 7. As we observe, there is a strong correlation between the two quantumness measures. Furthermore, the Wigner negativity correlates well with the test error of the experiment.

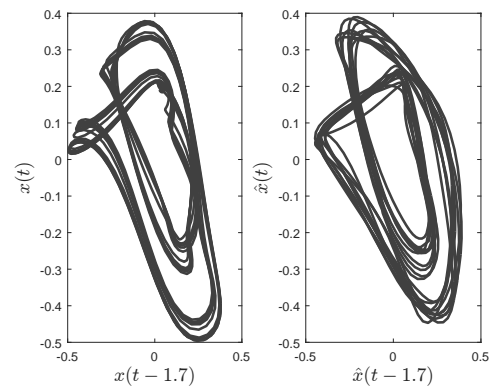
B. NOISE

Noise is an inevitable factor in quantum devices, and it is of profound importance for a quantum computing approach to be robust to noise. We show the robustness of this approach by considering different noise models as explained below.

Dephasing, Pumping, and the White noise. We introduce a dephasing error by considering the Lindbladian operators $L_n = \lambda |n\rangle \langle n|$. As observed in the experiments, this will not affect the results as much. Furthermore, the incoherent pumping error is simulated by considering the Lindbladian corresponding to λa^\dagger . On top of those, we add white noise to the input of the reservoir. This is performed via changing the equations of evolution (2) through the substitution $f(t) \rightarrow f(t) + \lambda' n(t)$. Here, $n(t)$ is the white noise of unit power, and λ' controls its strength. Fig. 8 shows the performance of the reservoir's output under both incoherent pumping, dephasing error, and white noise (see Eq. (2)). We have set $(K, \kappa, \alpha, \lambda, \lambda') = (0.05, 0.15, 1.2, 0.05, 0.02)$.



(a) Prediction of Mackey-Glass under the effects of noise. The noise models considered are dephasing incoherent pumping, and white noise on the input.



(b) Comparing the delayed embedding of the actual Mackey-Glass (left) with the reservoir's output (right) in the noisy settings.

FIG. 8: Noisy reservoir learning MG. The MG training process is performed when there are a variety of noises applied to the reservoir.

It is worth mentioning that noise in the context of reservoir computing is shown to be useful in certain cases [62, 63].

C. PROOF OF THEOREM 1

Recall the Gaussian integrals, which we will use at the end

$$\begin{aligned} \int_{\xi \in \mathbb{R}} e^{-\frac{\xi^2}{a^2}} d\xi &= \sqrt{\pi a^2}, \\ \int_{\xi \in \mathbb{R}} \xi^2 e^{-\frac{\xi^2}{a^2}} d\xi &= \frac{a^2}{2} \sqrt{\pi a^2}. \end{aligned} \quad (11)$$

Note that for any coherent state $|\alpha\rangle$, one has

$$W_\alpha = \frac{1}{\pi} e^{-[(x - \text{Re}(\alpha))^2 + (p - \text{Im}(\alpha))^2]}$$

Let us consider a set of K coherent states, namely $\{\rho_i = |\alpha_i\rangle\langle\alpha_i| : i = 1, 2, \dots, K\}$, and define $x_i := \text{Re}(\alpha_i)$, $p_i := \text{Im}(\alpha_i)$. Also let $(q_i)_{i \in [K]}$ be a probability distribution over K objects. We can then consider the mixture of coherent states as

$$\rho = \sum_{i=1}^K q_i |\alpha_i\rangle\langle\alpha_i|$$

since the Wigner function is linear with respect to the density matrix, one has

$$W_\rho(x, p) = \sum_{i=1}^K q_i W_{\alpha_i}(x, p)$$

Hence, we get

$$\begin{aligned} \frac{1}{\pi} I(\rho) &= \int_{x,p} \left(\sum_{i \in [K]} q_i \partial_x W_i(x, p) \right)^2 \\ &\quad + \left(\sum_{i \in [K]} q_i \partial_p W_i(x, p) \right)^2 \\ &\quad - 2 \left(\sum_{i \in [K]} q_i W_i(x, p) \right)^2 \\ &= \sum_{i,j \in [K]} q_i q_j \int_{x,p} \left(\partial_x W_i \partial_x W_j \right. \\ &\quad \left. + \partial_p W_i \partial_p W_j - 2W_i W_j \right) \end{aligned}$$

note that the terms in the summation above with $i = j$ could be rewritten as $q_i^2 I(\rho_i) = 0$ since any coherent state ρ_i has zero quantumness i.e., $I(\rho_i) = 0$. Furthermore, Claim 1 below guarantees that for any choice of i, j the expression in the parenthesis is non-positive, and hence, the proof is complete.

Claim 1. For any two coherent states, say $|\alpha_0\rangle$ and $|\alpha_1\rangle$, both of the following inequalities hold

$$\begin{aligned} \int_{x,p} \left(\partial_x W_0 \partial_x W_1 - W_0 W_1 \right) &\leq 0 \\ \int_{x,p} \left(\partial_p W_0 \partial_p W_1 - W_0 W_1 \right) &\leq 0 \end{aligned} \quad (12)$$

Proof. One has

$$W_0 = \frac{1}{\pi} e^{-[(x-x_0)^2 + (p-p_0)^2]}$$

hence

$$\begin{aligned} \partial_x W_0 &= -2 \frac{(x-x_0)}{\pi} e^{-[(x-x_0)^2 + (p-p_0)^2]}, \\ \partial_p W_0 &= -2 \frac{(p-p_0)}{\pi} e^{-[(x-x_0)^2 + (p-p_0)^2]} \end{aligned}$$

and similar expressions for W_1 and its derivatives. Let us now prove the first inequality. Define

$$\mathcal{A} := \int_{x,p} \left(\partial_x W_0 \partial_x W_1 - W_0 W_1 \right)$$

then, by direct substitution one gets

$$\begin{aligned} \mathcal{A} &= \frac{1}{\pi^2} \int_{x,p} (4(x-x_0)(x-x_1) - 1) \\ &\quad \times e^{-[(x-x_0)^2 + (x-x_1)^2 + (p-p_0)^2 + (p-p_1)^2]} \end{aligned}$$

we may now use the elementary identities $(x-x_0)(x-x_1) = (x - \frac{x_0+x_1}{2})^2 - (\frac{x_0-x_1}{2})^2$ and $(x-x_0)^2 + (x-x_1)^2 = (x - \frac{x_0+x_1}{2})^2 + (\frac{x_0-x_1}{2})^2$ and further, letting $\Delta x := x_0 - x_1$, $\Delta p = p_0 - p_1$, and $\bar{x} := \frac{x_0+x_1}{2}$, and $\bar{p} = \frac{p_0+p_1}{2}$ to conclude

$$\begin{aligned} \mathcal{A} &= \frac{e^{-\frac{1}{2}(\Delta x^2 + \Delta p^2)}}{\pi^2} \\ &\quad \times \int_{x,p} [4(x-\bar{x})^2 - (\Delta x)^2 - 1] \\ &\quad e^{-2(x-\bar{x})^2 - 2(p-\bar{p})^2} \\ &= -\frac{e^{-\frac{1}{2}(\Delta x^2 + \Delta p^2)}}{2\pi} (\Delta x)^2 \leq 0 \end{aligned}$$

(for the last equality, we use the Gaussian integrals in Eq. (11)). A similar argument gives the second inequality of the claim. \clubsuit

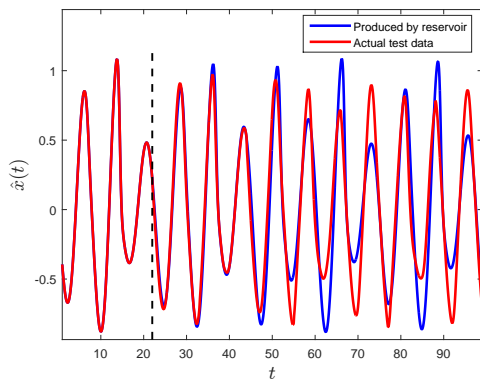
Supplementary Material for: Correlations Between Quantumness and Learning Performance in Reservoir Computing with a Single Oscillator

I. RÖSSLER ATTRACTOR

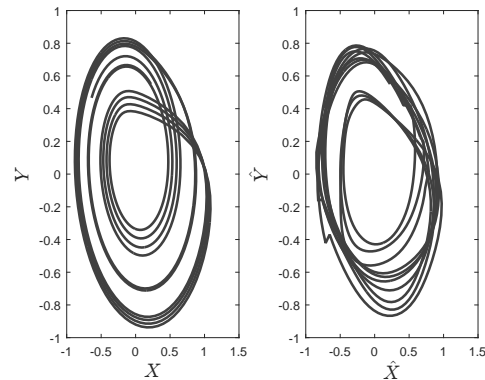
This section provides the performance in the training of Rössler attractor. The Rössler attractor [S64, S65] is a three-dimensional motion following the dynamics

$$\begin{cases} \frac{dx}{dt} &= -y - z \\ \frac{dy}{dt} &= x + ay \\ \frac{dz}{dt} &= b + z(x - c) \end{cases} \quad (\text{S1})$$

where $(a, b, c) \in \mathbb{R}^3$ are constant parameters, which we set to $(0.2, 0.2, 5.7)$ in our experiment. Fig. S1a and Fig. S1b show the model's learning results for this chaotic time series. We highlight that each component of the oscillator is learned independently from the others.



(a) The oscillator is trained to reproduce the Rössler time series, and then asked to perform prediction, given initial values, which are the data points before the dashed line. The parameters are $(\alpha, \kappa, K) = (1.0, 0.2, 0.01)$.



(b) Comparing the phase diagrams $X - Y$ of the Rössler attractor of the actual Rössler attractor with the predicted by the reservoir (left) with that of the reservoir's output (right).

FIG. S1: Rössler attractor training with a quantum oscillator.

II. MORE ON NOISE

In this section, we investigate the effect of adding white noise on the input to the reservoir. This error is introduced by the change equations of evolution through the substitution $f(t) \rightarrow f(t) + \lambda n(t)$. Here, $n(t)$ is the white noise of unit power, and λ controls its strength. Firstly, we consider a white noise applied to the input to the reservoir. Fig. S3 shows the outcome of learning noisy period functions. Despite significant signal distortion caused by noise, the oscillator demonstrates the ability to learn the underlying periodic functions. We further investigated the effect of training sawtooth signal with different noise levels, which resulted in Fig. S2. A similar experiment, this time with the MG, resulted in a training error of 0.053. Noting that the training error in the noiseless case results in an error of 0.047, we conclude that the model is robust to this noise model for a variety of prediction tasks. We made the choice of parameters $\alpha = 0.1$, $\kappa = K = 0.05$ in obtaining the results.

III. EVOLUTION ANIMATIONS

Animations showing the evolution of the Wigner function throughout the process are prepared and made available online at <https://github.com/arsalan-motamedi/QRC/tree/main/EvolutionAnimations>.

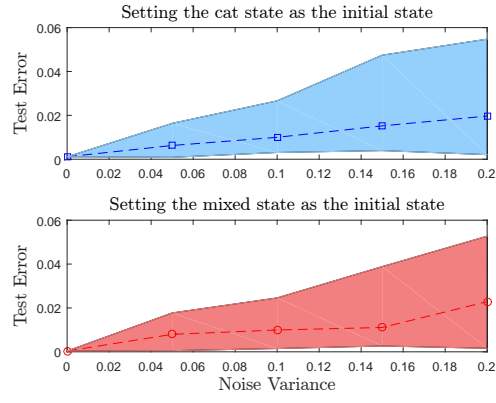


FIG. S2: Test error of training noisy sawtooth function. The initial states are the cat state and its classical mixture i.e., the normalized $|\alpha\rangle + |-\alpha\rangle$ and $|\alpha\rangle\langle\alpha| + |-\alpha\rangle\langle-\alpha|$. The noise model in this example is an additive white noise to the input.

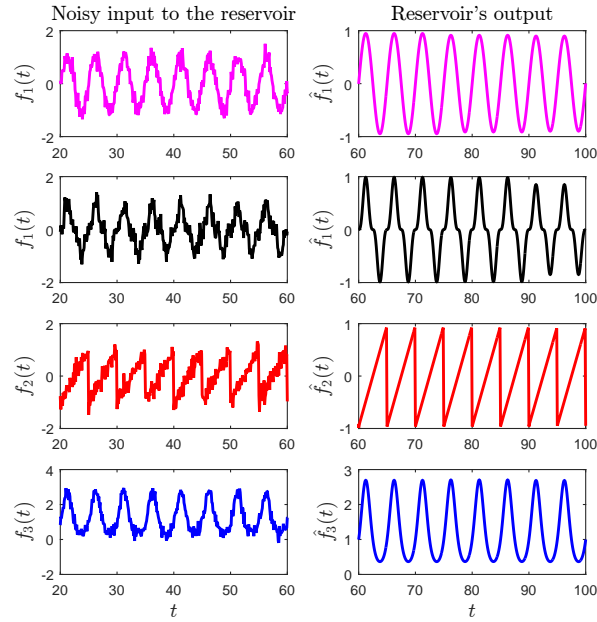


FIG. S3: Learning noisy periodic functions. The input to the reservoir is contaminated by white noise. However, the reservoir is still able to learn the input signal.